Melt compatibility between polyolefins: Evaluation and reliability of interfacial/surface tensions obtained by various techniques

Cédric Samuel, Thibault Parpaite, Marie-France Lacrampe, Jérémie Soulestin, Olivier Lhost

Melt Compatibility Between Polyolefins: Evaluation and Reliability of Interfacial/Surface Tensions Obtained by Various Techniques

Cedric Samuel[1,2*], *Thibault Parpaite*[1,2], *Marie-France Lacrampe*[1,2], *Jeremie Soulestin*[1,2], *Olivier Lhost*[3]

[1]Ecole Nationale Supérieure Mines Télécom Lille Douai (IMT Lille Douai), Department of Polymers and Composites Technology & Mechanical Engineering, 941 rue Charles Bourseul, 59508 Douai, France

[2]Université de Lille, 59000 Lille, France

[3]Total Research and Technology Feluy, Zone industrielle Feluy C, 7181 Seneffe, Belgium

*Corresponding author: cedric.samuel@imt-lille-douai.fr

Abstract

The interfacial tension in the melt state represents a key parameter to quantify the compatibility of polymer blends processed by extrusion techniques. Its evaluation is still challenging for polyolefin-based blends and, here, two complementary techniques (*i.e.* rheological and optical methods) were tested to evaluate the PP/PE compatibility in the melt state. In particular, interfacial/surface tensions at 200°C between several types of isotactic polypropylene (iPP) and polyethylene (PE) (*i.e.* Ziegler Natta- and metallocene-catalyzed grades) are specifically addressed to detect slight modifications of melt compatibility and to potentially highlight the role of polymer structure induced by the used catalyst. Classical dynamic rheology experiments coupled with morphological analyses were first attempted and several trends are clearly observed in term of iPP/PE interfacial tensions. iPP/metallocene PE associations display the lowest interfacial tension (0.9 – 1.2 mN/m, relative standard deviation ≈ 20%) and as-selected metallocene PE clearly gave rise to an enhanced melt compatibility with iPP matrices. Interfacial tensions could not be directly and precisely evaluated by optical methods using the polymer-in-polymer pendant drop method due a poor precision arising from an ultra-low iPP/PE melt density difference. However, surface tensions in the melt state obtained by the pendant drop method under nitrogen atmosphere represent the most reliable tool with an excellent sensitivity to as-selected polyolefin catalysts. An indirect but precise insight on polyolefin compatibility was found possible using surface tensions with a full discrimination between as-selected polyolefins in agreement with enhanced melt compatibilities in metallocene iPP/metallocene PE blends.

Key Words: Polymer Blends, Polyolefins, Interfacial Tension

1. Introduction

Polyethylene (PE) and polypropylene (PP) represent the most common thermoplastic polymers with colossal production rates up to 29 billion tons for 2016 in Europe (48.5% of the total polymer production)[1]. PE and PP are widely used in packaging, automotive, building and electronic industries to produce a large range of useful items (bags, bottles, containers, pipes, films, automotive parts, etc…). These unique figures for PE and PP mainly arise from their exceptional mechanical properties, low production cost and availability in a wide range of grades for most of processing technologies of the plastic industry[2].

Associations of polyolefins using melt extrusion techniques have been intensively considered to modify final properties at reasonable production costs. PP/PE associations in the melt state yield PP/PE blends and/or layered films with improved mechanical/impact properties (especially at low temperatures) for automotive and packaging applications with a possible use of recycled materials. Final properties of PP/PE blends depend on their compatibility and, in the realm, isotactic PP (iPP) and high-density polyethylene (HDPE) are immiscible and poorly-compatible in the melt state[3–8]. iPP/HDPE blend morphologies, final properties and impact of processing conditions were widely investigated by numerous authors. Characteristic matrix-droplet or co-continuous morphologies are observed and iPP/HDPE often displayed fragile mechanical behaviors with poor impact properties. Several compatibilizers such as poly(ethylene-*co*-propylene) elastomer[3], poly(ethylene-*co*-propylene-*co*-diene)[9,10]and poly(ethylene-*co*-vinyl acetate)[9] were tested for iPP/HDPE with moderate success.

The development of metallocene-catalyzed iPP (miPP) and PE (mPE) grades drastically changed the situation with significant and unexpected improvements of high industrial and scientific interests. The most famous investigation was proposed by Bates F. and coworkers on iPP/PE laminated films followed by characterizations of the delamination strength using T-peel tests[11]. The benefit of metallocene-catalyzed polyolefins was clearly highlighted with outstanding

interfacial strengths between miPP and mPE largely exceeding conventional combinations of Ziegler-Natta-catalyzed polyolefins. Hiltner A. and al. corroborated these results on co-extruded iPP/mPE films[12–14] and large improvements of impact properties were also observed for miPP/mPE blends[15–18]. The enhanced compatibility between metallocene-catalyzed polyolefins is ascribed to the quality of the miPP/mPE interface formed during melt processing. Large interdiffusion lengths across the interface are observed by transmission electron microscopy (TEM) and atomic force microscopy (AFM)[11–13,18,19] enabling efficient miPP/mPE entanglements and peculiar crystallization effects at the interface.

The melt compatibility between two polymers could be quantified by various physical parameters and especially surface/interfacial tensions in the melt state with (in)direct connections to interdiffusion lengths, solubility parameters[20–25] and various intrinsic thermodynamic properties[26–28]. Experimental data about surface/interfacial tensions are documented for several common iPP/PE grades[21,26,29–33] but remains unknown for metallocene-catalyzed polyolefins. Actually, the catalytic/initiating systems and conditions used for ethylene/propylene polymerization could control macromolecular parameters of as-produced polyolefins[2,34] and a precise prediction of surface/interfacial tensions of polyolefins is theoretically possible based on macromolecular parameters[24,25,31,32,34,35] (*i.e.*molecular weights &distributions, branch lengths&densities, nature of end-chain groups). Interfacial tensions and subsequent melt compatibility are expected to vary with respect to polyolefin grades in iPP/PE blends and such data could be of high academic and industrial interests for future predictions for the iPP/PE blend behavior. However, discriminant, precise and reliable experimental tools are required for iPP/PE systems.

The following study consequently deals with the evaluation of the iPP/PE melt compatibility (in particular for metallocene miPP and mPE grades) by means of interfacial/surface tensions in the melt state. Rheological and optical methods are selected for this purpose and iPP/PE interfacial tensions will be first captured by a classical rheological method coupled with morphology analysis

of iPP/PE blends (*i.e.* PE droplet size dispersed into iPP matrices). Optical methods by the pendant drop technique are then proposed in order to provide a better discrimination between iPP and PE grades regarding their blend compatibility. The reliability and sensitivity of each method is also discussed in order to extract information regarding iPP/PE melt compatibility.

2. Experimental section

2.1 Materials

Three polyethylenes (PE) and two isotactic polypropylenes (iPP) were kindly supplied by Total (Feluy, Belgium) and their physico-chemical properties are listed in **Table 1** and **Table 2**. Radical PE (rPE), Ziegler-Natta PE (zPE) and metallocene PE (mPE) grades were used with a constant melt flow index (MFI, determined at 190°C and 2.16kg for as-selected PE). A Ziegler-Natta isotactic PP (ziPP) and a metallocene isotactic PP (miPP) were also chosen with a constant MFI (determined at 230°C and 2.16kg for as-selected PP).

Table 1: Physico-chemical and macromolecular properties of selected PE grades.

	MFI (g/10min)	Density	M_n (Da)	M_w (Da)	M_z(Da)	M_w/M_n	M_z/M_n	T_m (°C)
rPE	7.5	0.918	16300	147000	688000	9.0	4.7	108
zPE	8.0	0.960	13100	65500	358000	5.0	5.5	134
mPE	8.5	0.960	19100	53200	101000	2.8	1.9	135

Table 2: Physico-chemical and macromolecular properties of selected PP grades.

	MFI (g/10min)	M_n (Da)	M_w(Da)	M_z(Da)	M_w/M_n	M_z/M_n	T_m (°C)
ziPP	25	32400	185000	562000	5.7	3.0	160
miPP	25	52800	157000	294000	3.0	1.9	150

2.2. Processing

iPP/PE blends were processed by twin-screw extrusion (Haake Rheomex PTW 16OS, Thermo Scientific, Germany, screw diameter 16mm, L/D 40) at 200°C with a screw speed of 100 rpm. iPP was chosen as the matrix with 20 wt-% PE as minor phase to generate PE droplets. Neat polymers and blends were then reprocessed into disks for rheology (diameter 35mm, thickness 2mm) by either compression molding (200°C, melting time 5min, low pressure cycle 4min, high pressure cycle 1min) or injection-molding (200°C, injection pressure 350 bar, mold temperature 30°C, holding time 10s).

2.3. Characterizations

2.3.1 Dynamic rheology

Dynamic rheology experiments were performed on iPP/PE blends and neat polymers using an Anton-Paar MCR301 dynamic rheometer equipped with plate-plate geometry (diameter 50mm, gap 1mm). Strain sweep at 200°C were first performed to verify the linear viscoelasticity range. Frequency sweeps at 200°C were then performed from 100 to 0.1 rad/s with a fixed strain to 10%.

2.3.2 Scanning electron microscopy

Morphologies of iPP/PE blends were determined by scanning electron microscopy (SEM) with a Leica SEM instrument operating at 15 kV. Compression-molded samples were cryo-fractured and coated with thin gold layer before SEM observations. Three zones of the cryo-fractured samples were scanned and processed into the image analysis software ImageJ. At least 50 droplets were measured on each image followed by droplet classification into 7-8 different size classes. The volume and number average size of the PE droplets in iPP matrices were determined using **equation 1–2,** based on the analysis of, for each blend, 3 images at various area of the sample

$$D_n = 2 \times \frac{\sum n_i \times R_i}{\sum n_i} \quad \textbf{(1)}$$

$$D_v = 2 \times \frac{\sum n_i \times {R_i}^4}{\sum n_i \times {R_i}^3} \quad \textbf{(2)}$$

with D_n the droplet number-average diameter, D_v the droplet volume-average diameter, R_i the average droplet radius of the *i*-class and n_i the number of droplets into the *i*-class.

2.3.3 Specific melt densities

Specific densities in the melt state are mandatory for surface/interfacial tension evaluation by optical methods. The specific volumes (and densities) in the melt state were accessed using a Goetfert capillary rheometer (Germany) equipped with a specific PVT device. The specific volume of the molten sample was acquired at 200°C and various pressures ranging from 20 to 120 bar. The specific melt densities at atmospheric pressure and 200°C was further obtained by extrapolation to 1 bar (0.1MPa). To insure the highest precision on specific volumes measurements at 200°C (in particular the absence of material leakage and bubbles), elastomeric sealants were changed for each material. The measurement routine was also repeated several times until reaching constant specific volumes. Average values with standard deviations were obtained from two experiments.

2.3.4 Melt-state pendant drop method

Surface and interfacial tensions were evaluated by the pendant drop method using a DSA100 goniometer (Krüss, Germany) equipped with a specific test chamber for high-temperature measurements. Neat polymers were extruded through a 2mm-diameter metal syringe and pendant drops of molten polymers with volumes ranging from 10 to 15 µL were formed at the die exit in a N_2 atmosphere. Molten drop profiles were recorded every 30s for 20min. Data were then processed with the DSA software to fit pendant drop profiles with a Young-Laplace model (**Figure 1** and **equation 3**) and access drop shape B-parameters and hence surface/interfacial tensions (**equation 4**). Drop shape parameters between 0.6 and 0.7 and accurate fits to the experimental drop profile are targeted for a good reliability of the surface/interfacial tensions. Two measurements were performed for each polymer and surface/interfacial tensions were taken as an average.

$$\frac{1}{R_1/a} + \frac{sin\varphi}{x/a} = B\frac{z}{a} + 2 \qquad \textbf{(3)}$$

$$B = \frac{\Delta\rho g a^2}{\gamma_L} \quad \textbf{(4)}$$

with Δρ the density difference between the two phases, *g* the Earth's gravity (9.81 m.s^{-2}), *a* the curvature radius at the apex and γ_L the surface tension of the pendant drop.

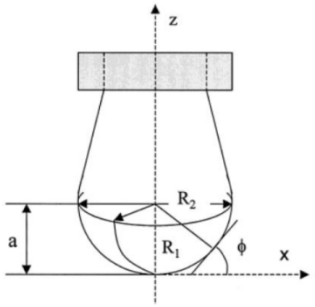

Figure 1: Ideal pendant drop profile for Young-Laplace fitting

2.3.3 Melt-state sessile drop method

Several surface tensions at 200 – 230°C were also approached by a sessile drop method. Polymer granulates (mass 10mg) were melted on various substrate at 230°C (PTFE, PDMS, PEI and PEEK) and contact angles were extracted from sessile drop profiles every 30s. Contact angles on each substrate were finally treated using an inverse Owens-Wendt plot with **equation 5** to get the overall surface tension with the dispersive and polar components.

$$\frac{1 + cos\theta}{\sqrt{\gamma_{sd}}} = \frac{2A}{(A^2 + B^2)} + \frac{2B}{(A^2 + B^2)}\frac{\sqrt{\gamma_{sp}}}{\sqrt{\gamma_{sd}}} \quad \textbf{(5)}$$

with A the square root of the dispersive component of the surface tension (γ_{pd}) for the molten polymer, B the square root of the polar component of the surface tension (γ_{pp}) for the molten polymer, Θ the contact angle between the sessile and the substrate, γ_{sp} the polar component of the surface tension for the substrate, γ_{sd} the dispersive component of the surface tension for the substrate.

3. Results and discussions

3.1 iPP/PE interfacial tension by the rheological method

The interfacial tensions at 200°C between various iPP/PE associations (and especially metallocene-catalyzed polyolefins) were first evaluated by a classical rheological method based on pioneer works by Palierne on the emulsion model of viscoelastic fluids[36]. Basically, the rheological behavior of polymer blends with matrix/droplet morphologies is marked by an extra-elasticity in the terminal regime (compared to the neat matrix), a behavior linked to mechanical droplet deformation and subsequent form relaxation. This relaxation process and its corresponding relaxation time (hereafter called droplet relaxation time) depend on various parameters such as droplet radius, viscosity ratio and the interfacial tension. Complex rheological models were further developed[37,38] but in a first approach the droplet relaxation time λ_{form} is given by **equation 6** developed by Gramespacher and Meissner[31,39]. In this respect, the rheological method could provide a direct access to γ_{12} and two important parameters need a careful evaluation, *i.e.* the droplet size (R) by SEM and droplet relaxation time (λ_{form}) by dynamic rheology (ϕ, η_m are constant and K is readily obtained, **Figure SI1**).

$$\lambda_{form} = \frac{R\eta_m}{4\gamma_{12}} \frac{(19K+16)[2K+3-2\phi(K-1)]}{10(K+1)-2\phi(5K+2)} \qquad \textbf{(6)}$$

with η_m the matrix newtonian viscosity, K the newtonian viscosity ratio, ϕ the volume fraction of dispersed phase and γ_{12} the interfacial tension.

Droplet sizes are critical to access the interfacial tension and this parameter was first approached using specific sample preparation/characterization techniques before rheology. Three iPP/PE blends (weight composition 80/20) were produced by twin-screw extrusion (miPP/mPE, ziPP/mPE and miPP/zPE) followed by compression-molding to insure a homogeneous, spherical and stable droplet morphology (droplet size stability was insured by a supplementary annealing treatment at 200°C, **Figure SI2**). Note that iPP and PE were used as a matrix and dispersed phase respectively due to viscosity considerations and avoid complex additional phenomenon such as in-situ fibrillation during processing[40]. For sake of comparison, an injection-molded blend was also

considered. Blend morphologies are displayed in **Figure 2** and matrix/droplet morphologies are clearly observed. Droplet sizes were determined after image analysis and results are listed in **Table 2**. Number-average diameters (D_n) between 2.3 – 2.7 µm and close to 1.2 µm were obtained for compression-molding and injection-molded samples, respectively. The polydispersity index (IP) clearly decreases after compression-molding, probably due to droplet coalescence at high residence time in the absence of shearing. Similar mPE droplet sizes are observed in ziPP and miPP matrices ($D_n \approx 2.3$ µm) but significant differences are detected with zPE droplets in miPP matrix ($D_n \approx 2.7$ µm). The interfacial adhesion is also improved by the use of mPE with a broad interface to the iPP matrix whereas partial debonding of zPE particles during cryofracture is observed attesting for a poor interfacial adhesion. These morphological features are in agreement with an enhanced melt compatibility in iPP/mPE systems.

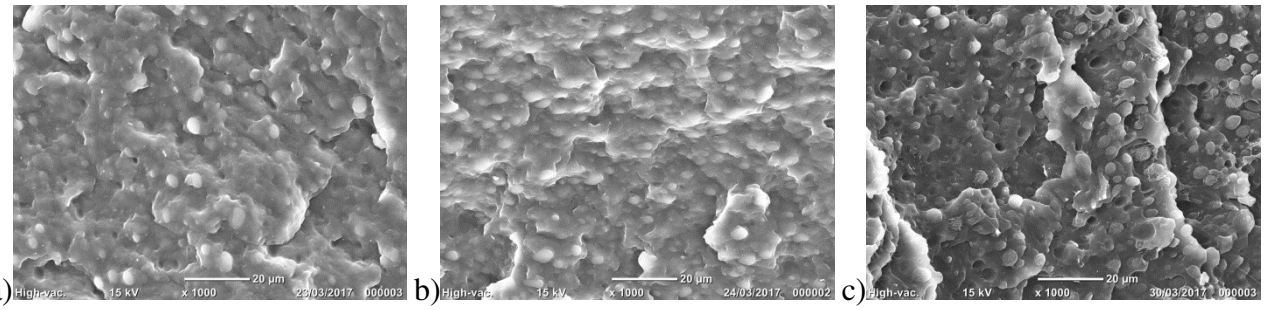

Figure 2: Morphologies of miPP/mPE (a), ziPP/mPE (b) and miPP/zPE (c) blends as observed by SEM on cryofractured and compression-molded samples (weight composition 80:20).

Table 2: Number-average (D_n), volume-average (D_v) and polydispersity (IP) of PE droplet diameters in considered iPP/PE blends (standard deviations into brackets according to **Figure SI3**).

Blend	D_n (µm)	D_v (µm)	IP
miPP/mPE[a]	2.3 (0.2)	3.0 (0.3)	1.28 (0.05)
ziPP/mPE[a]	2.3 (0.2)	2.9 (0.2)	1.25 (0.04)
ziPP/mPE[b]	1.2 (0.1)	1.8 (0.1)	1.61 (0.06)
miPP/zPE[a]	2.7 (0.3)	3.8 (0.2)	1.39 (0.10)

[a] Blends made by extrusion followed by thermocompression-molding.

[b] Blends made by extrusion followed by injection-molding.

Rheological analyses were then performed at 200°C and storage moduli as a function of the frequency are depicted in **Figure 3a-c**. Two relaxation peaks are systematically observed with a high-frequency peak for the matrix terminal relaxation and a low-frequency peak for the droplet relaxation. The droplet relaxation time $\lambda_{form\text{-}max}$ needs to be extracted from the peak position corresponding to droplet relaxation for the final computation of the interfacial tension γ_{12}. Several methods are available, *i.e.* the weighted relaxation time spectrum obtained by a regularization method developed by Honerkamp J. and Weese J. (**Figure 4a**)[30,41] and the imaginary part of the complex viscosity (**Figure 4b**) documented by Xu et al. for PLA/PBS blends[42]. The advantage of the latter method lies in the absence of any curve fitting and $\lambda_{form\text{-}max}$ ($=1/\omega_{form\text{-}max}$) could be readily obtained from experimental results but lower droplet relaxation times are obtained (**Table 3**) (probably due the absence of weighing effects, **Figure SI4-5**). The number-average droplet radius (R_n) was specifically considered for this latter method and similar interfacial tensions are reported for the two methods (**Table 3**). From a general point of view, iPP/PE interfacial tensions between 0.9 to 1.9 mN/m are detected for the blends, in accordance with previous investigations on iPP/HDPE (γ_{12} close to 2.2 mN/m at 200°C)[25,30,31]. An interesting trend is clearly captured with a significantly lower interfacial tension for blends based on mPE (0.9 – 1.2 mN/m) compared to blends based on zPE (1.6 – 1.9 mN/m), in agreement with recent investigations on the enhanced compatibility between metallocene polyolefin blends[11–13,18,19]. A good reliability of our calculated interfacial tensions is consequently concluded with a potential discrimination between mPE and zPE in terms of melt compatibility to iPP.

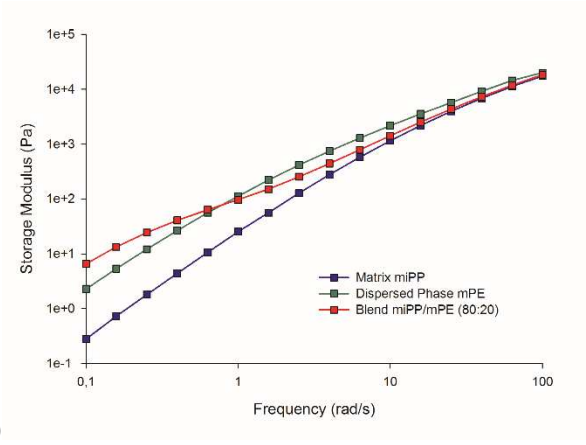

a)

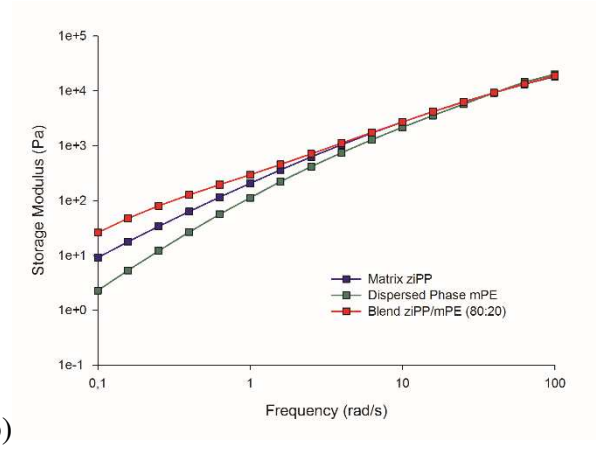

b)

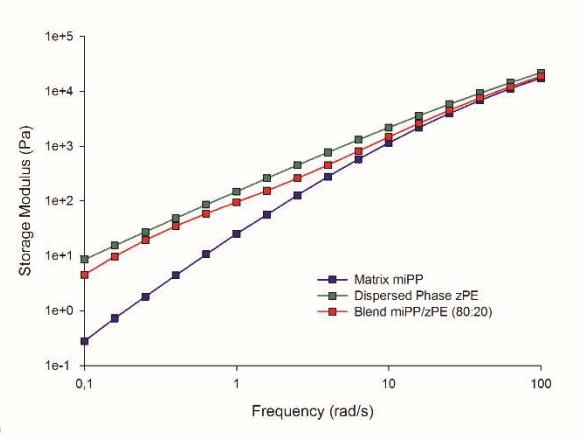

c)

Figure 3: Storage modulus as function of the frequency at 200°C for miPP/mPE (a), ziPP/mPE (b) and miPP/zPE (c) blends with related data for neat polymers.

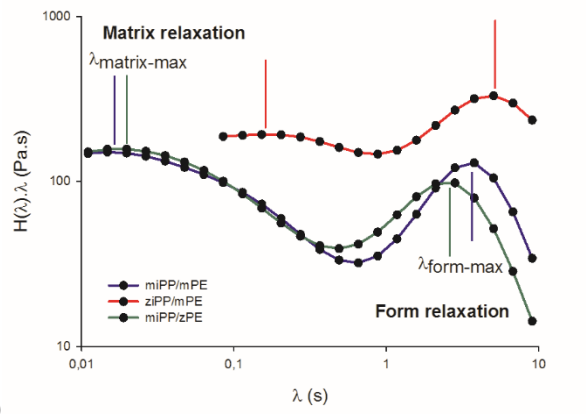

a)

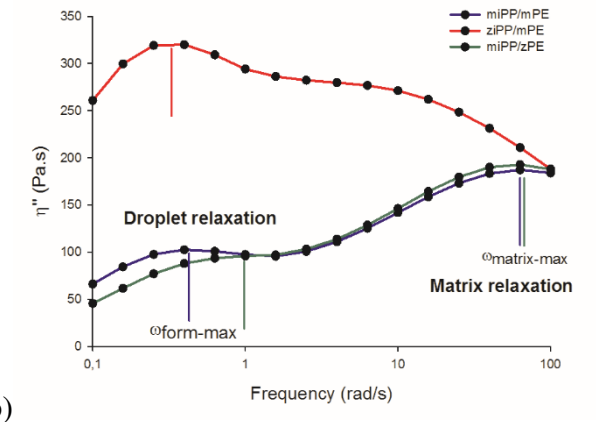

b)

Figure 4: Weighted relaxation spectra (a) and imaginary part of the complex viscosity as function of the frequency (d) at 200°C for all considered blends.

Table 3: Form relaxation time, newtonian viscosity ratio, matrix newtonian viscosity and interfacial tension for as-studied PP/PE blends.

Blend	$\lambda_{form\text{-}max}$ (s)[c]	$\lambda_{form\text{-}max}$ (s)[d]	K	η_m (Pa.s)	γ_{12}(mN/m)[c]	γ_{12}(mN/m)[d]
miPP/mPE[a]	3.6	2.4	2	585	0.9	1.0
ziPP/mPE[a]	4.9	3.3	1	1150	0.9	1.0
ziPP/mPE[b]	2.1	1.6	1	1150	1.2	1.1
miPP/zPE[a]	2.5	1.5	2.1	585	1.6	1.9

[a] Blends made by extrusion followed by thermocompression-molding.

[b] Blends made by extrusion followed by injection-molding.

[c] Obtained from the weighted relaxation spectra using weight-average droplet diameter.

[d] Obtained from the imaginary part of the complex viscosity using number-average diameter.

To strengthen above conclusions on iPP/PE interfacial tensions, the precision of these values was approached. The relative standard deviation (SD) on interfacial tensions arises from (i) the relative SD on droplet size and (ii) the relative SD on the droplet relaxation time (for other parameters such as newtonian viscosity, SD is rather low and could be neglected). For droplet size, according to **Table 2**, the relative SD on D_n and D_v could be set to approx. 10% based on 3 successive SEM analyses on various areas of cryo-fractured samples. For droplet relaxation time, the relative SD is linked to the evaluation of the low-frequency peak position and could be set to half the interval between experimental points. In this respect, the method based on the weighted relaxation spectrum provides the best precision and, for droplet relaxation time close to 3.6 s (droplet relaxation time measured for the miPP/mPE blend), the SD could be estimated to approx. 0.4 s for a relative SD on droplet relaxation time close to 10%. The global precision on the interfacial tension in iPP/PE blends by the rheological could be estimated close to 20% as the sum of the two relative SD, in agreement with previous estimations by Souza A.M.C et al. for iPP/PE blends [25,30,31]. Note this precision is also consistent the interfacial tension measured on a ziPP/mPE blend processed by injection-molding ($\gamma_{12} \approx 1.1 – 1.2$ mN/m) instead of compression-molding ($\gamma_{12} \approx 0.9 – 1.0$ mN/m). As a conclusion, the rheological method could easily discriminate mPE and zPE in terms of melt

compatibility to iPP with a significantly lower interfacial tension for iPP/mPE blends compared to iPP/zPE. However, only trends are captured by the rheological method in these iPP/PE systems and quantification of the interfacial tension is only possible with a precision close to 20%. In-depth discrimination between miPP and ziPP is actually not possible by this method. The main drawbacks of the rheological method lie in (i) the droplet size detection by image analysis of cryo-fractured samples and (ii) peculiar low-frequency behaviors with the related high extra-elasticity (elasticity even higher than neat polymers). More precise interfacial tension values and subsequent trends were attempted using optical methods by pendant drop techniques.

3.2 iPP/PE interfacial tensions by optical method

To validate above trends found by rheology, optical methods are good interests for a direct quantification of the interfacial tension in the melt state[43], in particular the polymer-in-polymer pendant drop method. However, polymer pairs required for this method should be carefully chosen in terms of specific melt densities and viscosities to insure (i) the establishment of a stabilized pendant drop profile in a moderate experimental time, (ii) a good optical contrast and (iii) a significant specific melt density difference $\Delta\rho$ (also called specific melt density contrast). In this respect, an evaluation of the specific melt density is mandatory and all materials were submitted to PVT experiments at 200°C for PE and 200 – 230°C for iPP. Specific melt densities at 200°C for our neat iPP/PE melts are comprised in the range 0.741 – 0.744 g/cm^3, with a classical decrease at higher temperatures for miPP and ziPP (**Table 4**). Only mPE seems to display a slightly higher specific melt density and the accuracy of the PVT method was checked with standard deviations evaluated to approx. 0.002 g/cm^3 on two successive measurements. Specific melt densities for LDPE, HDPE and iPP were also extracted from several studies found in literature (**Table 4**). Slightly lower specific densities are observed for the materials of the present study (**Table 4**) attributed to intrinsic errors related to PVT measurements using a capillary rheometer (material/barrel temperature difference, zero displacement calibration and/or material degradation at

long residence times). In this context, it could be stated out that the specific melt density contrast $\Delta\rho$ between our iPP and mPE is extremely low, even below detection levels for most of iPP/PE associations.

Table 4: Experimental specific melt densities at atmospheric pressure (0.1MPa) for as-selected iPP/PE in this study and values extracted from literature (average values, standard deviations into brackets).

Material	Specific density (g/cm^3) @ 200°C	Specific density (g/cm^3) @ 230°C	Ref
rPE	0.743	n.d.	
zPE	0.741	n.d.	
mPE	0.744 (0.002)	n.d.	
ziPP	0.741	0.725	
miPP	0.742 (0.002)	0.727(0.002)	
LDPE	0.753 (0.002)	n.d.	[36,37]
HDPE	0.757 (0.002)	n.d.	[36,37,38]
iPP	0.754 (0.002)	0.739 (0.003)	[37,39,40]

Taking into account the low specific density contrasts $\Delta\rho$, only two iPP/PE associations could be of interest for polymer-in-polymer pendent drop experiments, *i.e.* miPP/mPE and ziPP/mPE. Pendant drops were consequently attempted and drop profiles are displayed in **Figure 5** for a mPE (ρ = 0.744 g/cm^3) drop in a miPP medium (ρ = 0.742 g/cm^3). Long stabilization times were required to reach an equilibrium state and complex pendant drop profiles without any classical "pear" shape were observed. These phenomena are probably related to the intrinsic viscoelastic properties of neat component and the low interfacial tension in this iPP/PE system. The optical contrast between the two phases is also another problem for automatic drop edge detection and all

these points obviously represent severe obstacles to a direct evaluation of the miPP/mPE interfacial tension by optical techniques. Drop profiles were manually extracted using the approach developed by Stauffer C.E.[49], a reliable method for nearly-round pendant drops. The interfacial tension is directly calculated from the density difference ($\Delta\rho$), the equatorial diameter of the drop (D_e) and a correction factor H (**equation 6**). Tabulated values of 1/H are available from the shape parameter S (**equation 7**) and the precision of this method is theoretically good (lower than 10%) as long as S is higher than 0.5.

$$\gamma_{12} = \frac{\Delta\rho \times g \times D_e^2}{\mathrm{H}} \quad \textbf{(6)}$$

$$\mathrm{S} = {}^{Ds}/_{De} \quad \textbf{(7)}$$

with D_s the drop diameter at a distance D_e of the apex.

S values close to approx. 0.49 – 0.51 are obtained insuring an accurate value of D_s and hence of 1/H value. Interfacial tension value ranging from 0.4 – 0.6 mN/m are obtained with a noticeable increase of γ_{12} with experimental time, an effect attributed the higher drop volume. This low γ_{12} range is in accordance with above-mentioned results by the rheological method. Actually, it could be noticed that the extremely low specific melt density contrast $\Delta\rho$ close to 0.004 – 0.003 g/cm^3 (± 0.002 g/cm^3) naturally give rise to a low accuracy on γ_{12} (precision close to 60%) for the considered iPP/PE system. In this context, the direct evaluation of the iPP/PE interfacial tension by polymer-in-polymer pendant drop method to discriminate iPP/PE melt compatibility is clearly subjected to a poor precision in iPP/PE systems due to poor specific melt density contrasts.

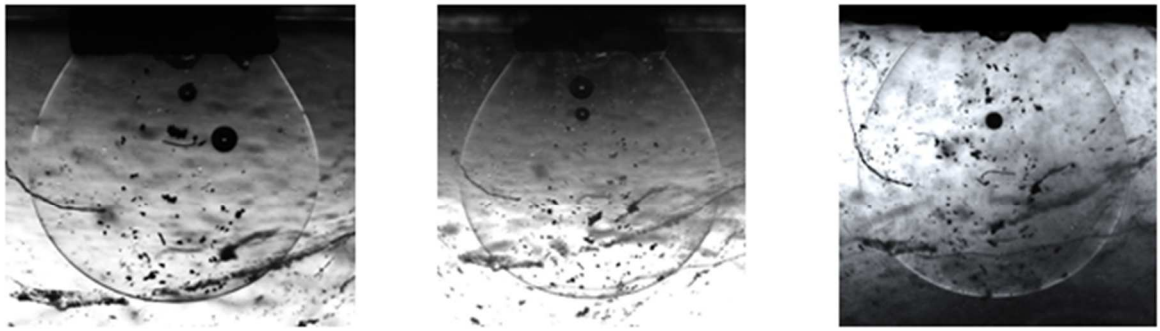

Figure 5: Experimental pendant drops of mPE in miPP at 200°C as a function of time.

3.3 iPP/PE surface tensions by optical method using pendant drops

The direct evaluation of the iPP/PE interfacial tension is clearly restricted and surface tensions of neat iPP/PE melts could be of goof interest to indirectly discriminate polyolefins in terms of melt compatibility. In this respect, pendant drops under N_2 atmosphere of neat zPE, rPE, mPE, ziPP and miPP at 200°C were attempted and displayed in **Figure 6**. A very good fit of the pendant drop profile is obtained using Young-Laplace equations (**equation 3 and 4**). Drop shape parameters B are listed in **Table 5** with values ranging from 0.65 to 0.69 insuring a very good quality of the surface tension measurements. It could be here noticed that mechanical equilibrium took place in approx. 10 - 15 min with as-chosen low-viscosity PE and iPP grades (MFI close to 25 for iPP and a MI2 close to 8 for PE). Surface tensions are tabulated in **Table 5** and a comparison between iPP/PE melts at 200°C is also attached in **Figure7** (PE was found very sensitive to thermal degradation/oxidation at 230°C and was only tested at 200°C). Surface tensions in the range 18 – 19 mN/m are obtained for iPP at 200°C with a classical decrease to 17 – 18 mN/m at 230°C. Trends between iPP/PE materials and impact of temperature are in accordance with many previous studies on polyolefin surface tension but lower values are systematically observed by approx. 2 – 3 mN/m[25,32]. This fact could be partly attributed to a reduced amount of additives in the PP/PE grades of the present study, in particular polar additives such as dibuthylphtalate[32].

A slightly lower value is obtained for ziPP with a difference by approx. 0.5 – 1.0 mN/m compared to miPP, an effect in accordance with the classical dependence of the surface tension on the number-average molar weight (32400 g/mol for ziPP compared to 52800 g/mol for miPP) [32]. For the surface tension of as-selected PE at 200°C, the situation is drastically different with large differences between PE grades. Surface tensions close at 23.1 and 21.8 mN/m for zPE and rPE were respectively measured, this trend is in accordance with surface properties of linear PE (or HDPE) and branched PE (or LDPE)[25]. Interestingly, the mPE grade is marked by a significantly low surface tension close to 21.4 mN/m and, to the best of our knowledge, this low value had never been documented. It could noticed that the classical dependence of the surface tension on the number-average molar weight is here no longer valid for PE and the origin of this discrepancy could found a potential origin on PE macromolecular structures (such as branching density and/or end-chain effects).

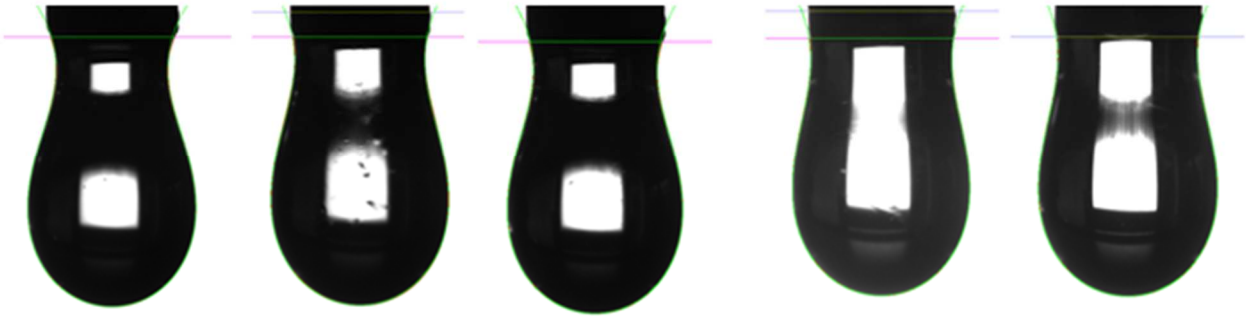

Figure 6: Pendant drop profiles at 200°C for zPE, rPE, mPE, ziPP and miPP (from left to right) (green line, Young-Laplace fitting of the detected shape profile).

Table 5: Surface tension and drop shape parameter (B) for as-studied PE and PP at 200 and 230°C (standard deviations into brackets).

Temperature (°C)	Material	Surface Tension (mN/m)	B
200	zPE	23.1 (0.3)	0.66

200	rPE	21.8 (0.3)	0.66
200	mPE	21.4 (0.4)	0.67
200	ziPP	18.3 (0.3)	0.68
200	miPP	19.1 (0.3)	0.68
230	ziPP	16.9 (0.5)	0.69
230	miPP	17.5 (0.4)	0.69

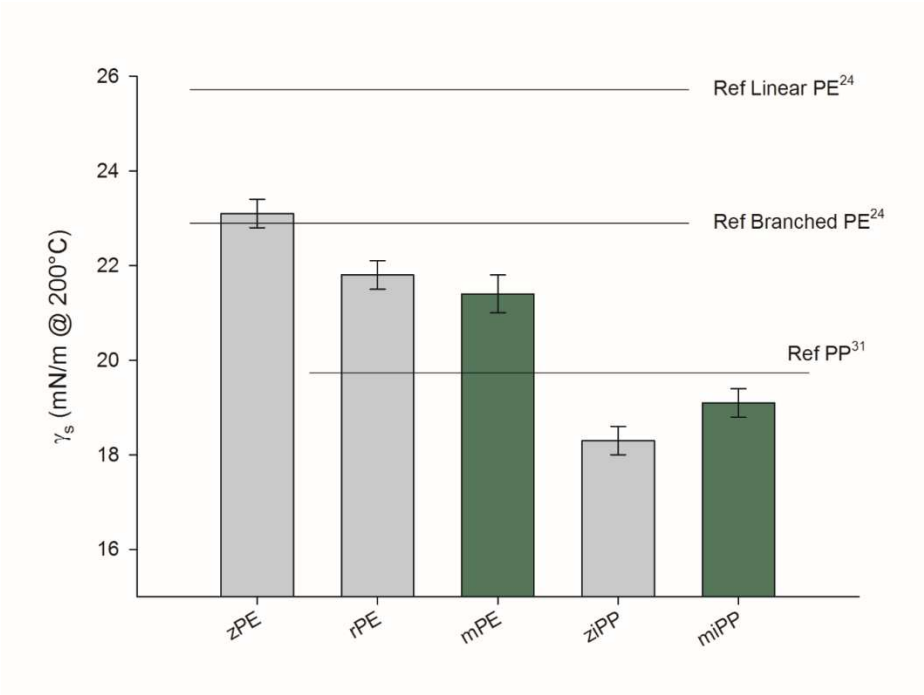

Figure 7: Comparisons of the surface tension for as-studied PE and PP at 200°C.

Concerning the precision/reliability of surface tension measurements, the standard deviation was evaluated to 0.3 – 0.5 mN/m based on several measurements. The precision on surface tension is consequently very high (relative SD close to 3% max.). In this respect, the closer miPP/mPE surface tension is confirmed with a surface tension difference as low as 2.3 mN/m (compared to 4.0 for miPP/zPE). From a surface tension point of view, the miPP/mPE association gives rise to the best melt compatibility, an effect only captured by the pendant drop technique under N_2 in the melt state.

As a conclusion, this technique represents the most sensitive and reliable tool to discriminate as-selected polyolefin grades and detect modifications of iPP/PE surface/interfacial properties.

3.3 iPP/PE surface tensions by optical method using sessile drops

Previous surface tensions by the pendant drop method under N_2 flow were corroborated by an Owen-Wendt approach using sessile drops. Contact angles between polyolefin melts and 4 different substrates are recorded at equilibrium and surface tensions with its dispersive and polar components could be approached using **equation 5**. **Figure 8** display the time-dependent contact angle at 230°C between a small ziPP granulate and poly(tetrafluoroethylene) (PTFE), poly(imide) (PI) and poly(dimethylsiloxane) (Silicone, PDMS). It could be observed that the contact angle fastly decreases with contact time to reach a stabilized value after 8 min for all substrates. Contact angles decreases in the order $\Theta_{ziPP/PTFE} > \Theta_{ziPP/PDMS} > \Theta_{ziPP/PI} > \Theta_{ziPP/PEEK}$. The same trends in terms of stabilization time and contact angle classification are also observed for miPP at 230°C. All contact angles are tabulated in **Table 6**. A characteristic inverse Owens-Wendt plot could be obtained for ziPP and miPP (**Figure 8**) and straight lines are roughly obtained with R^2 values close to 0.9. Surfaces tensions of ziPP and miPP were extracted and listed in **Table 6** with their dispersive and polar components at 230°C. By comparison with **Table 5**, good correlations between the pendant drop method and the sessile drop method are concluded with small discrepancies by 0.5 mN/m. Trends between ziPP and miPP is here also captured together with a very low polar component (< 2%) in accordance with the chemical nature of polyolefins, a parameter that could be only captured by sessile drop techniques. Interestingly, this method does not require the specific melt density to access surface tension but most of uncertainties mainly arise from surface tensions of substrates at the considered temperatures that give rise to poor correlation factors R^2 of the Owens-Wendt plot. However, surface tensions of ziPP and miPP accessed by the sessile drop method clearly validate previous surface tensions obtained by the pendant drop method and hence the improved compatibility between mPE and miPP.

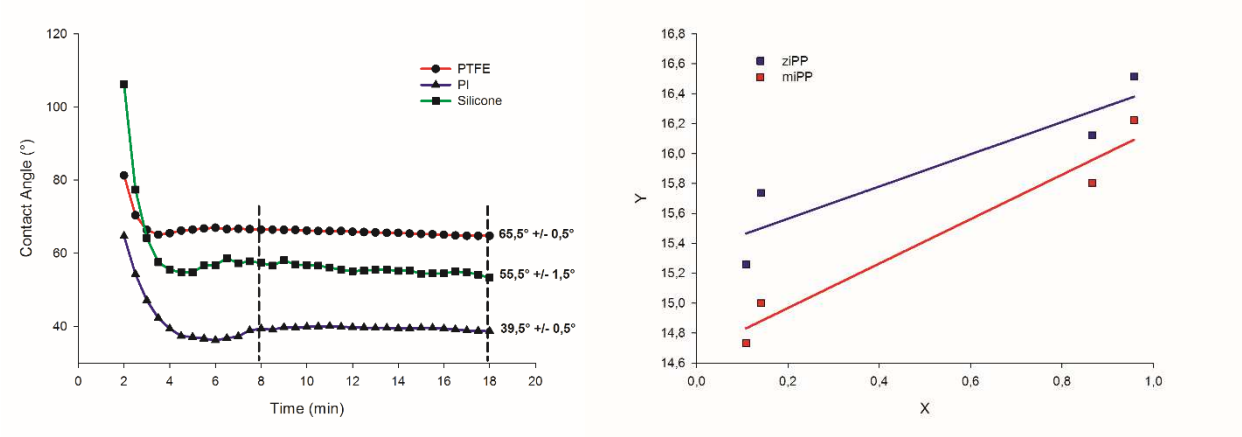

Figure 8: Evolution of the contact angle on various substrates for ziPP at 230°C (left) and inverse Owens-Wendt plot for ziPP and miPP at 230°C (right).

Table 6: Contact angle on various substrates, surface tension and polarity of as-studied PP at 230°C (sessile drop mass 10mg, standard deviation for contact angles +/- 1°).

Temperature (°C)	Material	Θ_{PTFE} (°)[a]	Θ_{PDMS} (°)[b]	Θ_{PI} (°)[c]	Θ_{PEEK} (°)[d]	Surface Tension (mN/m)	Polarity (%)[e]
230	ziPP	66	55	40	36	16.7	1
230	miPP	69	60	43	39	18.0	2

[a] For PTFE, γ^p = 8.5 mN/m and γ^d = 0.1 mN/m

[b] For PDMS, γ^p = 10.0 mN/m and γ^d = 0.2 mN/m.

[c] For PI,γ^p = 12.0 mN/m and γ^d = 9.0 mN/m.

[d] For PEEK, γ^p = 12.0 mN/m and γ^d = 11.0 mN/m.

[e] Polarity = $\gamma^p_{polymer}/\gamma^s_{polymer}$

3.4 Discussion

Table 7 gathers main results about surface/interfacial tensions between as-selected PP and PE with global comments regarding the precision of each method to capture/discriminate iPP/PE surface/interfacial tension (and hence in term of melt compatibility). For the rheological method, a direct access to the interfacial tension between polyolefins is possible with a precision close to 20%

by a careful analysis of the droplet relaxation times and droplet sizes. The rheological method clearly discriminates miPP/mPE and miPP/zPE blends with an enhanced compatibility of mPE in iPP matrices. However, ziPP and miPP matrices cannot be discriminated by the rheological method. The polymer-in-polymer pendant drop method should be clearly avoided to determine the interfacial tension in polyolefin blends since the melt density contrast between iPP and PE is extremely small with large difficulties associated to drop edge/shape detection. The pendant drop technique in N_2 does not give a direct access to interfacial tension but surface tensions in the melt state could be precisely evaluated with an accuracy close to 3%. This technique clearly represents the most sensitive and powerful technique to detect slight variations of surface properties with precise discriminations between miPP/ziPP grades and mPE/rPE/zPE grades. In this context, the surface tension difference between PE and PP ($\gamma_{s\text{-}PE} - \gamma_{s\text{-}PP}$) obtained by the pendant drop method could be viewed as the most precise quantitative indicator to investigate polyolefin compatibility in the melt state. Finally, it could be mentioned that the improved melt compatibility in the as-selected miPP/mPE blend is only captured by surface tension measurements, a trend particularly consistent with literature data related to laminated miPP/mPE bilayered films and to miPP/mPE blends [11–17]. Surface tension measurements by the pendant drop technique consequently represent a critical tool for (i) future investigations about the role of polymerization catalysts, conditions and induced structures on polyolefin melt compatibility and (ii) future selection/screening of suitable polyolefin grades for melt blending processing without the use of any compatibilizers.

Table 7. Comparison between experimental techniques to evaluate iPP/PE melt compatibility.

Technique	Comments
Rheological method	• Direct access to the interfacial tension with precision close to 20% • Discrimination possible between mPE and zPE • γ_{12} (miPP/mPE) ≈ 0.9 – 1.2 mN/m

	• γ_{12} (miPP/zPE) ≈ 1.6 – 1.9 mN/m
Pendant drop method (polymer-in-polymer)	• Direct access to interfacial tension but poor precision due to ultra-low melt density contrast • γ_{12} (miPP/mPE) ≈ 0.4 – 0.6 mN/m
Pendant drop method (under N_2 atmosphere)	• Only access to surface tension but high precision (approx. 3%) and high sensitivity to polyolefin types • Discrimination possible between ziPP (γ_s ≈ 18.3 mN/m) and miPP (γ_s ≈ 19.1 mN/m) • Discrimination possible between mPE (γ_s ≈ 21.4 mN/m) and zPE (γ_s ≈ 23.1 mN/m)

Conclusions

The proposed work highlights the efficiency of various tools (rheological and optical methods) to quantify the melt compatibility between polyolefins by means of surface/interfacial tensions in the melt state. The PP/PE interfacial tension at 200°C was directly and successfully evaluated by a rheological method (frequency sweeps coupled to microscopic analyses) and a discrimination between miPP/mPE and miPP/zPE associations was possible (γ_{12} ≈ 0.9 – 1.0 mN/m against 1.6 – 1.9 mN/m respectively, precision close to 20%). As-selected metallocene polyethylene clearly gave rise to an enhanced melt compatibility to iPP in accordance with recent studies on such associations. Optical methods were then tested to increase the precision over the interfacial tension but the polymer-in-polymer pendant drop method should be avoided in polyolefin systems. However, the surface tension obtained by the pendant drop method in N_2 was found extremely precise (precision close to 3% and sensitive to PP/PE grades. All as-selected materials were easily discriminated in terms of surface tensions at 200°C with peculiar surface tensions were detected for mPE and miPP, an mPE/miPP association also marked by the lowest surface tension difference. The surface tension

difference could consequently represent a precise quantitative parameter for future evaluation/optimization/prediction of the melt compatibility between polyolefins using melt-based process in the absence of any compatibilizers.

Acknowlegments

This research was financially supported by Total S.A.. Authors gratefully acknowledge both the International Campus on Safety and Intermodality in Transportation (CISIT, France), the European Community (FEDER funds) as well as the Hauts-de-France Region (France) for their contributions to funding extrusion equipments and characterization tools (dynamic rheometers, microscopes and goniometers).

Data availability

The raw and processed data required to reproduce these findings are available on request to corresponding author.

References

[1] Plastics Europe - Association of Plastics Manufacturers, Plastic - the Facts 2016, (2016).

[2] P. Galli, G. Vecellio, Polyolefins: The Most Promising Large-Volume Materials for the 21st Century, J. Polym. Sci. Part A Polym. Chem. 42 (2004) 396–415.

[3] D.W. Bartlett, J.W. Barlow, D.R. Paul, Mechanical Properties of Blends Containing HDPE and PP, J. Appl. Polym. Sci. 27 (1982) 2351–2360.

[4] H.P. Blom, W. Teh, A. Rudin, iPP/HDPE Blends: Interactions at lower HDPE Contents, J. Appl. Polym. Sci. 58 (1995) 995–1006.

[5] J.W. Teh, A. Rudin, J.C. Keung, A review of polyethylene–polypropylene blends and their compatibilization, Adv. Polym. Technol. 13 (1994) 1–23.

[6] S. Jose, A.S. Aprem, B. Francis, M.C. Chandy, P. Werner, V. Alstaedt, S. Thomas, Phase morphology, crystallisation behaviour and mechanical properties of isotactic polypropylene/high density polyethylene blends, Eur. Polym. J. 40 (2004) 2105–2115.

[7] U.A. Handge, K. Okamoto, H. Münstedt, Recoverable deformation and morphology after uniaxial elongation of a polystyrene/linear low density polyethylene blend, Rheol. Acta. 46 (2007) 1197–1209.

[8] C.M. Tai, R.K.Y. Li, C.N. Ng, Impact behaviour of polypropylene / polyethylene blends, Polym. Test. 19 (2000) 143–154.

[9] H.P. Blom, J.W. Teh, A. Rudin, iPP/HDPE Blends. II. Modification with EPDM and EVA, J. Appl. Polym. Sci. 60 (1996) 1406–1417.

[10] K.P. Tchomakov, B.D. Favis, M.A. Huneault, M.F. Champagne, F. Tofan, Mechanical Properties and Morphology of Ternary PP/EPDM/PE Blends, Can. J. Chem. Eng. 83 (2008) 300–309.

[11] K.A. Chaffin, J.S. Knutsen, P. Brant, F.S. Bates, High-Strength Welds in Metallocene Polypropylene/Polyethylene Laminates, Science 288 (2000) 2187–2190.

[12] B.C. Poon, S.P. Chum, A. Hiltner, E. Baer, Adhesion of polyethylene blends to polypropylene, Polymer 45 (2004) 893–903.

[13] B.C. Poon, S.P. Chum, A. Hiltner, E. Baer, Modifying Adhesion of Linear Low-Density Polyethylene to Polypropylene by Blending with a Homogeneous Ethylene Copolymer, J. Appl. Polym. Sci. 92 (2004) 109–115.

[14] A.M. Jordan, K. Kim, F.S. Bates, C.W. Macosko, S. Jaffer, O. Lhost, Rheological characterization and thermal modeling of polyolefins for process design and tailored interfaces, AIP Conf. Proc. 1843 (2017) 0–4.

[15] A.P. Gupta, V. Gupta, U.K. Saroop, Morphological and Impact Properties of Thermo-oxidative Degraded Polypropylene/Metallocene Linear Low Density Polyethylene Blend Systems, Polym. Plast. Technol. Eng. 46 (2007) 759–766.

[16] K.A. Chaffin, F.S. Bates, P. Brant, G.M. Brown, Semicrystalline blends of polyethylene and isotactic polypropylene: Improving mechanical performance by enhancing the interfacial

structure, J. Polym. Sci. Part B Polym. Phys. 38 (2000) 108–121.

[17] K.A. Chaffin, F.S. Bates, P. Brant, Semicrystalline polymer blends, 2000.

[18] A.M. Jordan, K. Kim, D. Soetrisno, J. Hannah, F.S. Bates, S.A. Jaffer, O. Lhost, C.W. Macosko, Role of Crystallization on Polyolefin Interfaces: An Improved Outlook for Polyolefin Blends, Macrolecules. 51 (2018) 2506–2516.

[19] A.C. Chang, S.P. Chum, A. Hiltner, E. Baer, Characterization of an amorphous surface layer on blown polyolefin film, J. Appl. Polym. Sci. 86 (2002) 3625–3635.

[20] P.J. Cole, R.F. Cook, C.W. Macosko, Adhesion between immiscible polymers correlated with interfacial entanglements, Macromolecules. 36 (2003) 2808–2815.

[21] M. Yamaguchi, Effect of molecular structure in branched polyethylene on adhesion properties with polypropylene, J. Appl. Polym. Sci. 70 (1998) 457–463.

[22] E. Helfand, Theory of inhomogeneous polymer. Lattice model for solution interfaces, J. Chem. Phys. 63 (1975) 2192–2198.

[23] E. Helfand, Y. Tagami, Theory of the interface between immiscible polymers, Polym. Lett. 9 (1971) 741–746.

[24] A. Ajji, L.A. Utracki, lnterphase and Compatibilization of Polymer Blends, Polym. Eng. Sci. 36 (1996) 1574–1585.

[25] S. Wu, Polymer interface and adhesion, M. Dekker. (1982).

[26] N.R. Demarquette, J.C. Moreira, R.N. Shimizu, M. Kamara, M.R. Kamal, Influence of temperature, molecular weight, and molecular weight dispersity on the surface tension of polystyrene, polypropylene, and polyethylene. II. Theoretical, J. Appl. Polym. Sci. 83 (2002) 2201–2212.

[27] G.T. Dee, B.B. Sauer, The cohesive energy density of polymers and its relationship to surface tension, bulk thermodynamic properties, and chain structure, J. Appl. Polym. Sci. 134 (2017) 1–14.

[28] B.B. Sauer, G.T. Dee, Surface tension and melt cohesive energy density of polymer melts including high melting and high glass transition polymers, Macromolecules. 35 (2002) 7024–7030.

[29] E.Y. Arashiro, N.R. Demarquette, Use of the pendant drop method to measure interfacial tension between molten polymers, Mater. Res. 2 (1999) 23–32.

[30] A.M.C. Souza, N.R. Demarquette, Influence of composition on the linear viscoelastic behavior and morphology of PP/HDPE blends, Polymer 43 (2002) 1313–1321.

[31] A.M.C. Souza, N.R. Demarquette, Influence of coalescence and interfacial tension on the morphology of PP / HDPE compatibilized blends, Polymer 43 (2002) 3959–3697.

[32] J.C. Moreira, N.R. Demarquette, Influence of temperature, molecular weight, and molecular weight dispersity on the surface tension of PS, PP, and PE. I. Experimental, J. Appl. Polym. Sci. 82 (2001) 1907–1920.

[33] A.T. Morita, D.J. Carastan, N.R. Demarquette, Influence of drop volume on surface tension evaluated using the pendant drop method, Colloid Polym. Sci. 280 (2002) 857–864.

[34] J.B.P. Soares, J.D. Kim, G.L. Rempel, Analysis and Control of the Molecular Weight and Chemical Composition Distributions of Polyolefins Made with Metallocene and Ziegler−Natta Catalysts, Ind. Eng. Chem. Res. 36 (1997) 1144–1150.

[35] E.Y. Arashiro, N.R.R. Demarquette, Influence of temperature, molecular weight, and polydispersity of polystyrene on interfacial tension between low density polyethylene and polystyrene, J. Appl. Polym. Sci. 74 (1999) 2423–2431.

[36] D. Graebling, R. Muller, J.F. Palierne, Linear Viscoelastic Behavior of Some Incompatible Polymer Blends in the Melt. Interpretation of Data with a Model of Emulsion of Viscoelastic Liquids, Macromolecules. 26 (1993) 320–329.

[37] U. Jacobs, M. Fahrländer, J. Winterhalter, C. Friedrich, Analysis of Palierne's emulsion model in the case of viscoelastic interfacial properties, J. Rheol. 43 (1999) 1495-1509.

[38] M. Bousmina, Rheology of polymer blends: Linear model for viscoelastic emulsions, Rheol. Acta. 38 (1999) 73–83.

[39] H. Gramespacher, J. Meissner, Interfacial tension between polymer melts measured by shear oscillations of their blends, J. Rheol. 36 (1992) 1127–1141.

[40] M. Yousfi, T. Dadouche, D. Chomat, C. Samuel, J. Soulestin, M.-F. Lacrampe, P. Krawczak, Development of nanofibrillar morphologies in poly(l -lactide)/poly(amide) blends: role of the matrix elasticity and identification of the critical shear rate for the nodular/fibrillar transition, RSC Adv. 8 (2018) 22023–22041.

[41] J. Honerkamp, J. Weese, Determination of the Relaxation Spectrum by a Regularization Method, Macromolecules. 22 (1989) 4372–4377.

[42] L.Q. Xu, H.X. Huang, Relaxation behavior of poly(lactic acid)/poly(butylene succinate) blend and a new method for calculating its interfacial tension, J. Appl. Polym. Sci. 125 (2012).

[43] P. Xing, M. Bousmina, D. Rodrigue, Critical Experimental Comparison between Five Techniques for the Determination of Interfacial Tension in Polymer Blends : Model System of Polystyrene / Polyamide-6, Macromolecules. (2000) 8020–8034.

[44] L. Capt, M.R. Kamal, The Pressure-Volume-Temperature Behavior Polyethylene Melts, Int. Polym. Process. 15 (2000) 83–94.

[45] P.A. Rodgers, Pressure Volume Temperature Relationships for Polymeric Liquids: a Review of Equation of State and their Characteristic Parameters for 56 Polymers, J. Appl. Polym. Sci. 48 (1993) 1061–1080.

[46] Y. Sato, H. Hashiguchi, K. Inohara, S. Takishima, H. Masuoka, PVT properties of polyethylene copolymer melts, Fluid Phase Equilib. 257 (2007) 124–130.

[47] R. Fulchiron, E. Koscher, G. Poutot, D. Delaunay, G. Régnier, Analysis of the Pressure Effect on the Crystallization Kinetics of Polypropylene: Dilatometric Measurements and

Thermal Gradient Modeling, J. Macromol. Sci. Part B Phys. 40 (2001) 297–314.

[48] Y. Sato, Y. Yamasaki, S. Takishima, H. Masuoka, Precise Measurement of the PVT of Polypropylene and Polycarbonate up to 330°C and 200 MPa, J. Appl. Polym. Sci. 66 (1997) 141–150.

[49] C.E. Stauffer, The Measurement of Surface Tension by the Pendant Drop Technique, J. Phys. Chem. 69 (1965) 1933–1938.

Graphical Abstract